Pure Appl. Chem., Vol. 82, No. 4, pp. 917–929, 2010.
doi:10.1351/PAC-CON-10-01-06

Mastering nanostructured materials through H-bonding recognitions at interfaces*

Stefan Mohnani[1,2], Anna Llanes-Pallas[1], and Davide Bonifazi[1,2,‡]

[1]Department of Pharmaceutical Sciences, University of Trieste, Piazzale Europa 1, I-34127, Trieste, Italy; [2]Department of Chemistry, University of Namur, Rue de Bruxelles 61, B-5000, Namur, Belgium

Abstract: The controlled engineering of functional architectures composed of π-systems with unusual opto-electronic properties is currently being investigated intensively from both fundamental research and technological application viewpoints. In particular, the exploitation of the supramolecular approach for the facile construction of multidimensional architectures, featuring cavities capable of hosting functional molecules, could be used in several applications, such as nanomedicine, molecular-based memory storage devices, and sensors. This paper highlights our recent strategies to use hydrogen-bonding interactions to prepare nanostructured functional architectures via the self-assembly of organic molecular modules studied at different interfaces.

Keywords: hydrogen bonding; interfaces; liquid–solid; liquid–liquid; nanopatterned surfaces; STM; supramolecular chemistry; self-assembly; UHV–solid; vesicles.

INTRODUCTION

The electronic, physical, and chemical properties of materials (such as metals, crystals, silicon, and mica) vary greatly depending on whether they are considered in the bulk entity or at the surface [1]. The difference is that in the bulk, atoms are arranged in an ordered periodic structure (e.g., a lattice in a crystal), whereas at a surface, atoms or molecules assume averaged equilibrium positions, different from those inside the crystal lattice, due to the absence of some of their neighbors. Consequently, at the surface, the structure, energy levels, and electronic properties of the atoms or molecules generally differ in comparison to those in a bulk entity. In all applications that involve an interface (i.e., the contact region between two immiscible phases), these differences in the properties between the "surface" and "bulk" are very important. In this respect, the creation of new materials based on organic molecules at interfaces and the investigation of their properties is a growing multidisciplinary field [2,3]. The increased development and knowledge in the mastering of organic chemistry, alongside improved deposition and analysis techniques, has led to a tendency towards the fabrication of functional nanoscale electronic devices based on organic molecules [4–15]. In order to build such devices, the development, understanding and mastering of fabrication methods for the controlled engineering of well-defined organic structures is fundamental to the research activities [16,17]. Thus, the precise control and understanding of molecule–substrate, and molecule–molecule interactions, as well as their structural properties are crucial parameters for both the construction of electronic [4,5,13–15,18–23] or biomedical [24,25] devices

Pure Appl. Chem.* **82, 757–1063 (2010). An issue of reviews and research papers based on lectures presented at the 13th International Symposium on Novel Aromatic Compounds (ISNA-13), 19–24 July 2009, Luxembourg City, Luxembourg on the theme of aromaticity.
‡Corresponding author: E-mail: davide.bonifazi@fundp.ac.be

and also, for fine-tuning their performances. Chemical modification of the organic molecules provides a promising tool for the adjustment of such properties. Therefore, state-of-the-art organic synthesis can lead to libraries of molecular modules that can subsequently be adsorbed on surfaces, and depending on the chemical nature of the molecule, the resultant devices' properties can be controlled in a predictable manner.

The "bottom-up" approach is possibly the most promising method to date for the construction of molecular-based devices. It involves the exploitation of multiple noncovalent interactions between the pre-engineered molecules, which through their selective recognition sites are able to form convergent assemblies [26–31]. Furthermore, the dynamicity of these supramolecular interactions allows the equilibrium to take place rapidly, leading toward thermodynamically stable structures. This is a favorable feature since the system can repair itself if errors arise in the assembly (so-called "self-repair"), consequently allowing for the formation (at the μm scale) of long-range ordered and defect-free systems that are barely achievable through conventional covalent synthesis. This also means that the preparation of the predetermined building blocks is facilitated since their synthesis requires significantly fewer steps than the covalent synthesis that would be necessary to prepare an analogous system [32–34]. One of the major considerations when working with materials that are organized at the molecular level for technological applications, is indeed the aforementioned fact that matter at this scale can no longer be considered as a bulk entity [35]. Furthermore, the role of the interface is not insignificant, and thus the surface's characteristics contribute to the final materials' properties. As a consequence, the most popular engineering method in nanotechnology is to deposit or modify the surfaces of bulk materials (e.g., metals, semiconductors, insulators, liquids) with organic molecules. The substrate may act simply as a mechanical support for the organic material, but sometimes it can also be exploited for a function, e.g., as a counter electrode. Following this approach, a large variety of regular one- and two-dimensional assemblies have been supramolecularly constructed on surfaces using the full spectrum of intermolecular interactions: hydrogen-bonding, dipole–dipole, donor–acceptor, van der Waals (vdW), and coordinative interactions. For examples of such assemblies, the readers are invited to read recent reviews in the field [36,37]. As described in the reviews, the main method of investigating surface-confined self-assembled molecular materials is by using scanning probe microscopy techniques. In particular, the invention of the atomic force and scanning tunnelling microscopies (AFM and STM, respectively) made it possible to generate images of molecule-based architectures adsorbed at surfaces in direct space with a nanometre-scale resolution [38–41].

In this review paper, an account of our advances in the last two years to prepare nanostructured architectures via the self-assembly of organic molecular modules at various interfaces will be discussed. The discussion will be limited to systems that we have constructed using H-bonding supramolecular interactions, giving rise to hollowed systems that could be subsequently exploited to host functional molecules.

MASTERING OF SELF-ASSEMBLED STRUCTURES AT INTERFACES

This part of the review is divided into three sections: self-assembly at the solid–liquid interfaces; self-assembly at the solid–vacuum interfaces; and self-assembly at liquid interfaces. The first two sections involve systems that were investigated using STM at atmospheric conditions and under ultra-high vacuum (UHV) conditions, respectively. It is important to understand the merits of each of these techniques in order to identify which one should be used for any given molecule under investigation. Under UHV conditions, substrate coverage can be controlled in a well-defined environment [42]. Furthermore, the mobility, and consequently, the assembly of the deposited molecules can be controlled by varying the temperature. This high level of control and the fact that the tunnelling current passes through a vacuum, rather than a medium with a higher dielectric constant, leads to extremely high-resolution images [43]. However, since the deposition of molecules onto the substrate under UHV conditions is performed by sublimation, the technique is limited to species with high thermal stability and limited size.

Investigations at the solid–liquid interface are performed at atmospheric conditions, therefore, these limitations do not exist, i.e., the restrictions related to the size and functional groups of the molecules that can be analyzed are far less stringent. Another advantage of performing STM at the liquid–solid interface is that the dynamic exchange of molecules between the surface and liquid phase promotes the repair of defects in the self-assemblies. A critical factor in obtaining good STM images with this technique is the choice of solvent. Ideally, the solvent should be nonconductive, should have a low vapor pressure, and should have a lower affinity for the substrate compared to the solute. Despite these advantages and disadvantages, both techniques have been extensively exploited in recent years to investigate supramolecular assemblies at interfaces. Our recent results utilizing both techniques are discussed below.

Self-assembly at the solid–liquid interfaces

Using approaches borrowed from the crystal engineering field, in one of our early collaborative works involving the solid–liquid interface, the controlled formation of a bicomponent porous network utilizing H-bonding was demonstrated [44]. The molecules used in the study were a bis-functionalized uracyl-bearing linear module (**1**) and melamine (**2**) (Fig. 1a). The two compounds were dissolved in 1,2,4-trichlorobenzene (TCB) and were deposited on highly oriented pyrolitic graphite (HOPG) surfaces. Initially, both molecules **1** and **2** were investigated individually on the HOPG surface. In each case, highly crystalline self-assembled monolayers were observed (Figs. 1b,c). However, when the two compounds were codeposited onto the HOPG surface, hexagonal porous network in two dimensions were observed (Figs. 1d,e). With its capacity to form nine H-bonds in total, melamine (**2**) directs the self-assembly by assuming the positions at the apices of the hexagons and interacting with three bis-uracyl units (**1**) through triple H-bonds with each one, as it is shown in Fig. 1a. These H-bonding interactions result in an angle of 120 ± 12º at the apex between two bis-uracyl units. It is noteworthy to point out that the porous network formed only at low concentrations (~2 μM), since at higher concentrations (~20 μM) only tightly packed monolayers of melamine (**2**) were observed. Thus, it was shown that by utilizing the low concentration regime, i.e., controlling the concentration, competitive

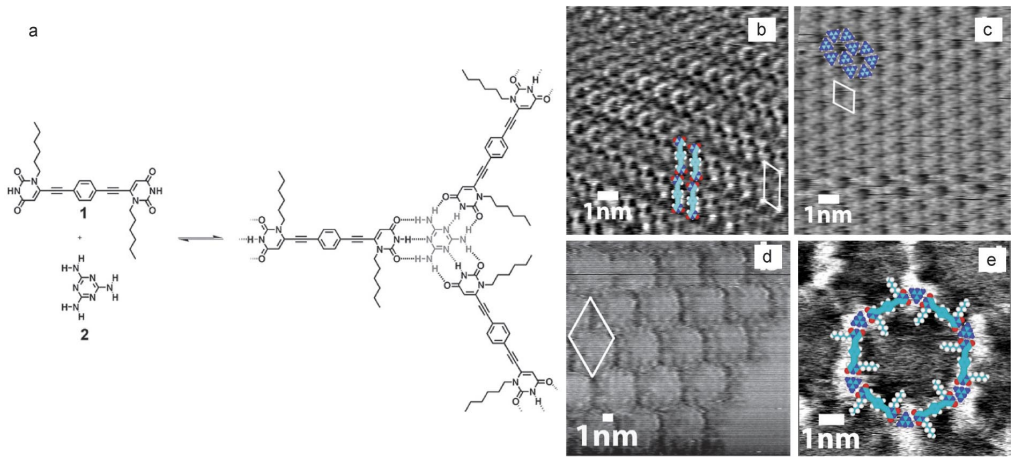

Fig. 1 (a) Chemical structures of bis-functionalized uracyl-bearing linear module (**1**) and melamine (**2**). Also, the equilibrium formation of the hybrid porous assembly via H-bonding interactions is shown; (b) STM image of the monocomponent self-assembly of **1**; (c) STM image of the monocomponent self-assembly of **2**; (d) STM image of the bicomponent self-assembly showing the hexagonal porous network formed; (e) The proposed assembly model is shown superimposed over a single hexagonal pore [44]. Adapted with permission from The Royal Society of Chemistry. Copyright © 2008.

physisorption between **1** and **2** at the HOPG–TCB interface could be prevented and submonolayer coverage could be achieved.

As an extension of the previous work, a comparative study of four linear linkers interacting with melamine units (**2**) via triple H-bonds was carried out [45]. This study offered new insight into the design and versatility of pre-programmable bicomponent supramolecular 2D networks at the solid–liquid interface. The ditopic imidic linkers included two molecules bearing diuracil groups in the α and ω positions, **1** and **3**, respectively, naphthalene tetracarboxylic diimide (**4**) and pyromellitic diimide (**5**) (Fig. 2a). The self-assembly of each linker with melamine was carried out by dissolving them in a solvent mixture of TCB/DMSO and subsequently depositing them on HOPG. By controlling the concentration and stoichiometry of the systems precisely, the formation of the desired bicomponent self-assembly could be favored. The STM imaging experiments revealed that two-dimensional porous architectures could be formed by three, out of the four linkers, when they were codeposited onto the

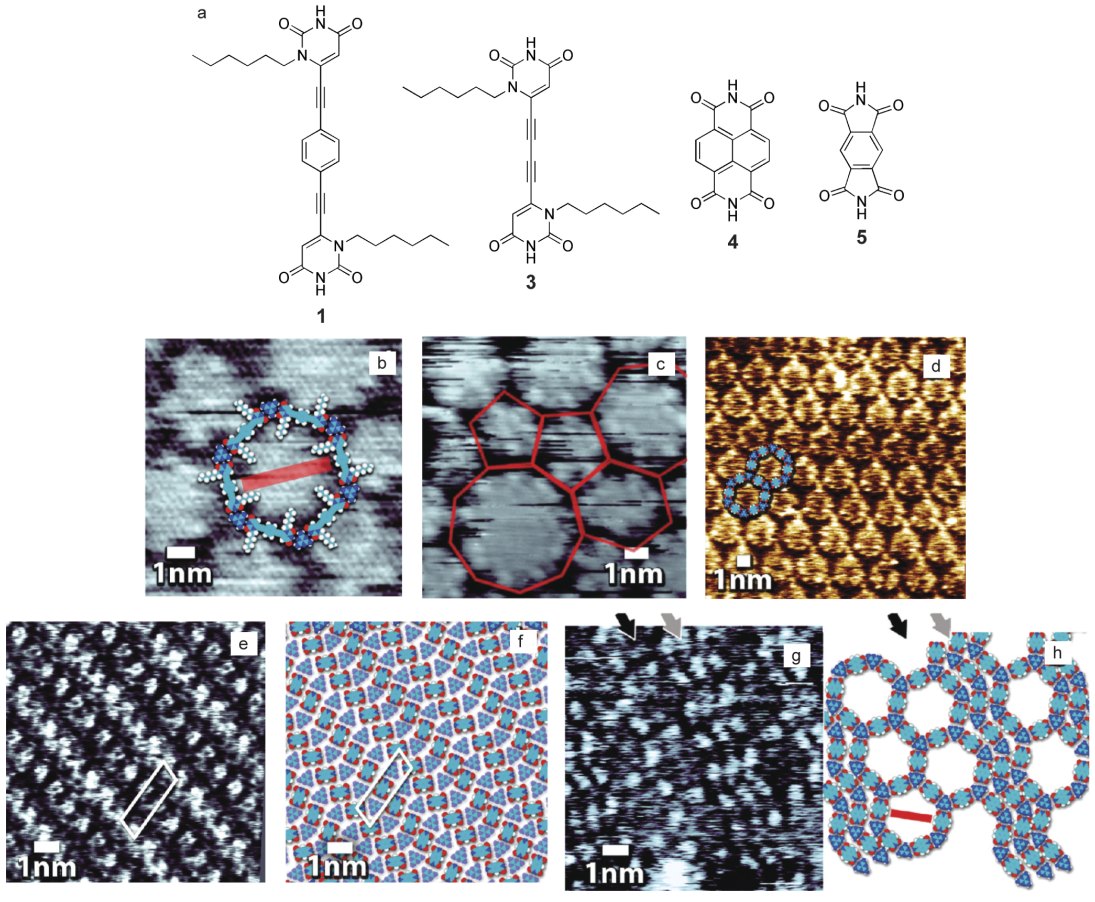

Fig. 2 (a) Chemical structures of the linear linkers used in the study; (b) STM image of the self-assembly formed by **1** and **2**. A molecular model of the hexagonal structure formed is superimposed. The bar corresponds to 3.2 nm; (c) STM image of the self-assembly formed by **3** and **2** showing that various polygons were formed; (d) STM image of the long range highly ordered hexagonal pattern formed by **4** and **2**; (e,f) STM image and molecular model of the tightly packed one-dimensional supramolecular arrays formed by **5** and **2**; (g,h) STM image and molecular model of the hexagonal porous networks coexisting with a one-dimensional supramolecular linear assembly formed at a lowered ratio of **2**:**4** compared to Fig. 2d. The linear-chain polymorph is indicated by the gray arrow, whereas the hexagonal motif is indicated by the black arrow [41]. Adapted with permission from the American Chemical Society. Copyright © 2009.

HOPG surface in the presence of **2**. With two of the linkers, molecules **1** and **4**, highly ordered hexagonal structures were obtained (Figs. 2b,d). The self-assembly between molecular modules **2** and **3** resulted in a distribution of various polygonal structures from pentagons to nonagons (Fig. 2c). The co-deposition of **5** with **2** resulted in tightly packed one-dimensional supramolecular arrays (Figs. 2e,f). When the stoichiometric ratio of **2** relative to **4**, was altered by lowering the concentration of **2**, it was observed that the hexagonal porous networks coexisted with one-dimensional supramolecular linear assemblies (Figs. 2g,h), thus demonstrating the importance of controlling the concentrations and stoichiometries of the molecular systems. In fact, the occurrence of multiple phases was observed for all the bicomponent systems with concentrations below 100 μM. This comparative study confirmed that a concentration-dependent polymorphism and phase segregation are hallmarks of porous self-assembled structures prepared via H-bonding interactions at solid–liquid interfaces [46,47]. Furthermore, the study also revealed several crucial points that have to be considered when designing a pre-programmed porous network at the molecular level. The rigidity of the linkers is very important. In the case of module **3**, for example, the diethynyl moiety introduces a fair amount of conformational flexibility, allowing the formation of polymorphic and glassy phases and thus is not an optimal choice when looking for a fully rigid molecular module. Peripheral functionalization of the linkers would prevent strong side-to-side interactions that lead to tightly packed bicomponent assemblies rather than porous networks and would also hinder strong adsorption in the cavities of the porous networks. Also, by designing the molecular modules in a multicomponent system with complementary recognition sites, phase segregation and self-recognition can be avoided. Furthermore, another manner of avoiding such polymorphism and phase segregation at solid–liquid interfaces is to introduce a guest at the cavities of a self-assembled porous network formed by H-bonding interactions as was shown by various groups [48–51]. Thus, it was shown that by careful investigation of the energetic contributions in crystallization, polymorphism, and phase segregation, a dramatic improvement in chemical design, and thus in the molecular engineering, can be achieved.

In another parallel study, further complexity was introduced to the molecular modules in order to attempt the formation of various potential polygonal porous domains (Fig. 3a) [52]. Two types of assembling molecular modules were prepared, 1,3,6,8-tetrakis[(1-hexylurac-6-yl)ethynyl]pyrene (**6**) and 4,4'-[(phen-1,4-diyl)diethynyl]bis(2,6-diacetylaminopyridine) (**7**) (Fig. 3b). The two modules feature required H-bonding sites to form the polygonal assemblies, with molecule **6** bearing uracilic moities similarly to **1** described above, whereas **7** is functionalized with two 2,6-di(acetylamino)pyridine groups to provide complementary H-bonding sites for the uracilic derivatives. The uracilic moities in tetratopic module **6** were oriented at 60º and 120º relative to each other, therefore this molecule would direct the geometry of the assembly. The two di(acetylamino)pyridyl groups in **7** were at 180º with respect to each other, thus allowing this module to act as the linear linker between the tetratopic modules. Following the submonolayer strategy to prevent competitive adsorption, it was possible to investigate the formation of discrete self-assemblies featuring polygonal porous domains at the solid–liquid interface (solvent: DMSO-TCB, surface: HOPG, r.t.). The discrete H-bonded assemblies were nucleated in solution and were studied at very low-concentrated solutions (<10 μM). Due to the difference in adsorption energies of the two components, and the tendency to minimize the occupied area by forming close-packed assemblies, it is very challenging to direct the deposition of two different molecules on a surface unless such low concentration conditions are used. Despite these difficulties, several polygon-like oligomeric species featuring hollow structures featuring the predesigned geometries of the constituent molecular modules were observed following deposition (Figs. 3c–f).

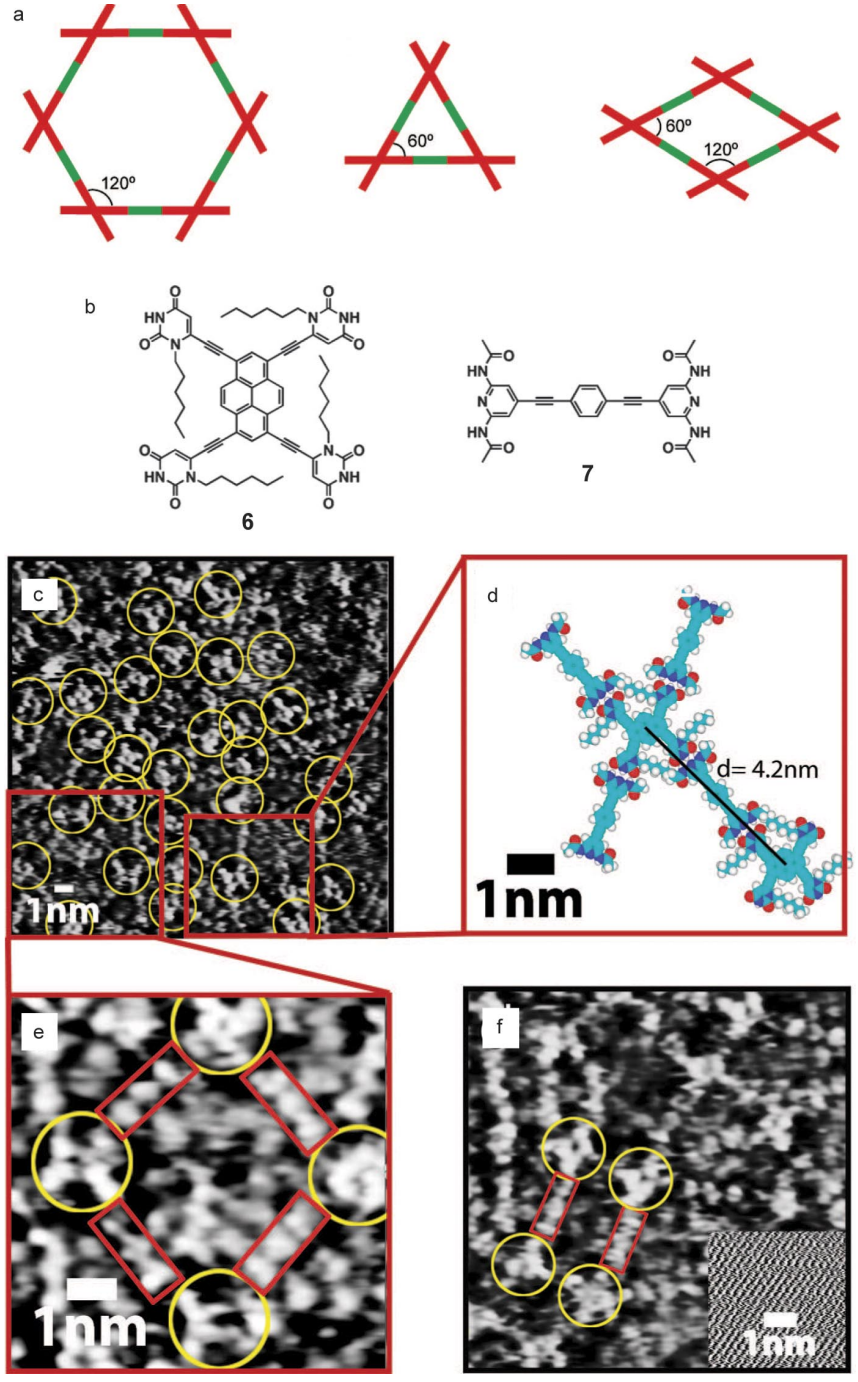

Fig. 3 (a,b) Chemical structures and polygonal assemblies of the molecular modules **6** and **7**; (c) Submolecularly resolved images featuring discrete oligomeric species $[(\mathbf{6})_m \cdot (\mathbf{7})_n]$ prepared from diluted equimolar solutions. Each circle identifies a single molecule of **6**; (d) Model assembly of a hexameric hybrid complex $[(\mathbf{6})_2 \cdot (\mathbf{7})_4]$ estimated by MM2-based computational geometry optimization; (e,f) Heterogeneous **6·7** phase images highlighting the presence of rhomboidal and rectangular nanopolygons. Each circle identifies a single molecule of **6** and each rectangle a single molecule of **7** [52]. Adapted with permission from the American Chemical Society. Copyright © 2009.

Self-assembly at the solid–vacuum interfaces

Our efforts to prepare nanostructured architectures on surfaces are not limited to the liquid–solid interface. Interesting results have also been obtained using related molecular modules under UHV conditions on metal surfaces. In a recent collaborative study using 4,4'-[(phen-1,4-diyl)diethynyl]bis(2,6-diacetylaminopyridine) (**7**, Fig. 3b), it was demonstrated that a porous network could be formed upon deposition of the molecular module on a Ag(111) surface [53]. Deposition of **7** at submonolayer coverages onto the Ag(111) surface at room temperature resulted in the self-organization into a porous hexagonal network (Fig. 4a). In Fig. 4b, it can be seen that each 2,6-di(acetylamino)pyridine moiety interacts via two H-bonds with equivalent neighboring residues, consequently resulting in a chiral hexameric units. Each cavity was surrounded by three molecules of **7** arranged at an angle of 60º with respect to each other. This gave rise to a rhombic unit cell (shown in Fig. 4b) with dimensions of 30.4×30.4 Å^2 and an angle of 60º. Astonishingly, annealing the sample to 420 K caused a phase transition, transforming the hexagonal porous network into a close-packed 2D rhombic arrangement (unit cell: 20.2×10.0 Å^2 with an angle of 68.2º, Figs. 4c,d).

The first clue to the cause of this dramatic change was provided by the fact that the intensity of the two acetyl units of terminal 2,6-di(acetylamino)pyridine moieties differed, with one of the residues appearing brighter than the other. This clearly indicated that there was a conformational difference between the two acetyl groups. An explanation for this phenomenon is that in principle the amidic functional groups can exist in both the *cis*- and *trans*-conformations, with the *trans* being preferred, as was the case in the hexagonal porous network. However, theoretical calculations (Fig. 4e) showed that the conformations could be switched if sufficient energy was provided. It was therefore postulated that following the annealing, one of the two acetyl units of the terminal 2,6-di(acetylamino)pyridine moieties was in the *cis*-conformation, with the other remaining in the *trans*-conformation, enabling the formation of four H-bonds (see Fig. 4e) between neighboring molecules in a head-to-head fashion. This H-bonding was designated as $(DADA)_2$ (where D refers to a H-bonding donor moiety and A refers to a H-bonding acceptor moiety) according to the scheme in Fig. 4e. These results showed that the hexagonal porous network was kinetically controlled, whereas the rhombic assembly was the thermodynamically stable phase.

In another set of experiments, a three-component assembly was prepared under UHV conditions [54]. The three molecular modules used are shown in Fig. 5a. Two of the modules, **1** and **7**, have been used in experiments described above, and a new module, an anthracene bearing a uracilic H-bonding moiety **8**, was introduced to act as a molecular stopper. Before attempting the three-component system, several assemblies were investigated for comparison purposes. First, **1** was deposited on Ag(111) and was investigated under UHV conditions at 77 K. At submonolayer coverages, two types of close-packed arrays were observed (Figs. 5b–d). It has to be noted that depending on the relative spatial disposition, the hexyl chains on the uracilic moities could display two configurations, *cis*-**1** or *trans*-**1**, where the alkyl chains lie on the same or opposite sides of the molecular backbone, respectively. In the first packing motif, two adjacent rows of *cis*-**1** interact via double head-to-head H-bonds using the uracil moities and also via vdW interactions between the alkyl chains to form molecular wires with double rows (Fig. 5c). In the second motif, two lateral rows of *cis*-**1** molecules are linked through *trans*-**1** molecules. The intermolecular interaction between the *trans*-**1** molecules with the *cis*-**1** molecules occurs via the interaction of the NH group of the *trans*-**1** molecules with the free carbonyl on the *cis*-**1** molecules (Fig. 5d). As expected, an attempt to assemble **1** and **8** resulted in disordered phases due to the lack of complementary H-bonding sites. On the other hand, sequential deposition of **1** and **7** resulted in the formation of very regular extended linear bimolecular wires, which were only disrupted at the terraces of the silver substrate (Figs. 5e–g). The two modules alternate to form the wires, with each molecule able to form two sets of triple H-bonds to interact with two neighbors using the pre-programmed complementary recognition groups DAD and ADA available on the 2,6-di(acetylamino)pyridine and uracilic residues on **7** and **1**, respectively. In this assembly, generally molecule **1** was found in the *cis*-**1** confor-

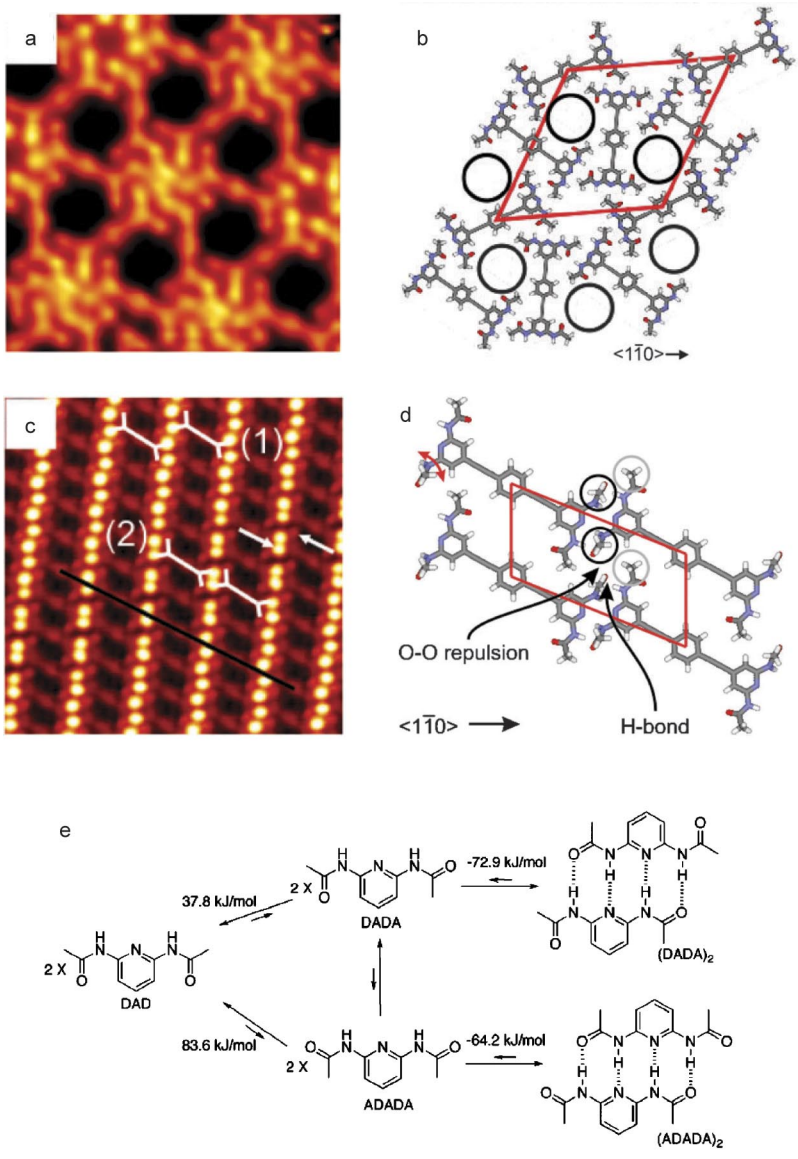

Fig. 4 (a,b) STM image (7×7 nm^2) and proposed model of the hexagonal porous network of **7** on Ag(111) at room temperature under UHV conditions; (c,d) STM image and proposed model of the close-packed rhombic pattern (10×10 nm^2) formed upon annealing at 420 K on Ag(111); (e) scheme showing the influence of the *cis*- and *trans*-conformers and calculated $\Delta H°$ for conformational changes and dimerization in the vacuum using MP2/6-311G** level of approximation on B3LYP/6-311G** [53]. Adapted with permission from The Royal Society of Chemistry. Copyright © 2009.

mation in order to minimize the free surface energy by forming the most densely packed arrangement possible. Indeed in this array, the trans-1 conformation was very rarely observed. Next, the three-component assembly was attempted by sequential sublimation of the three modules onto the Ag(111) surface. In this case, the extended wires imaged between **1** and **7** were not observed. As predicted, the monouracil conjugate **8**, acted as a molecular stopper exposing the anthracyl moiety as the end point of the assembly preventing the molecular wires from reaching the terraces of the silver substrate as occurred

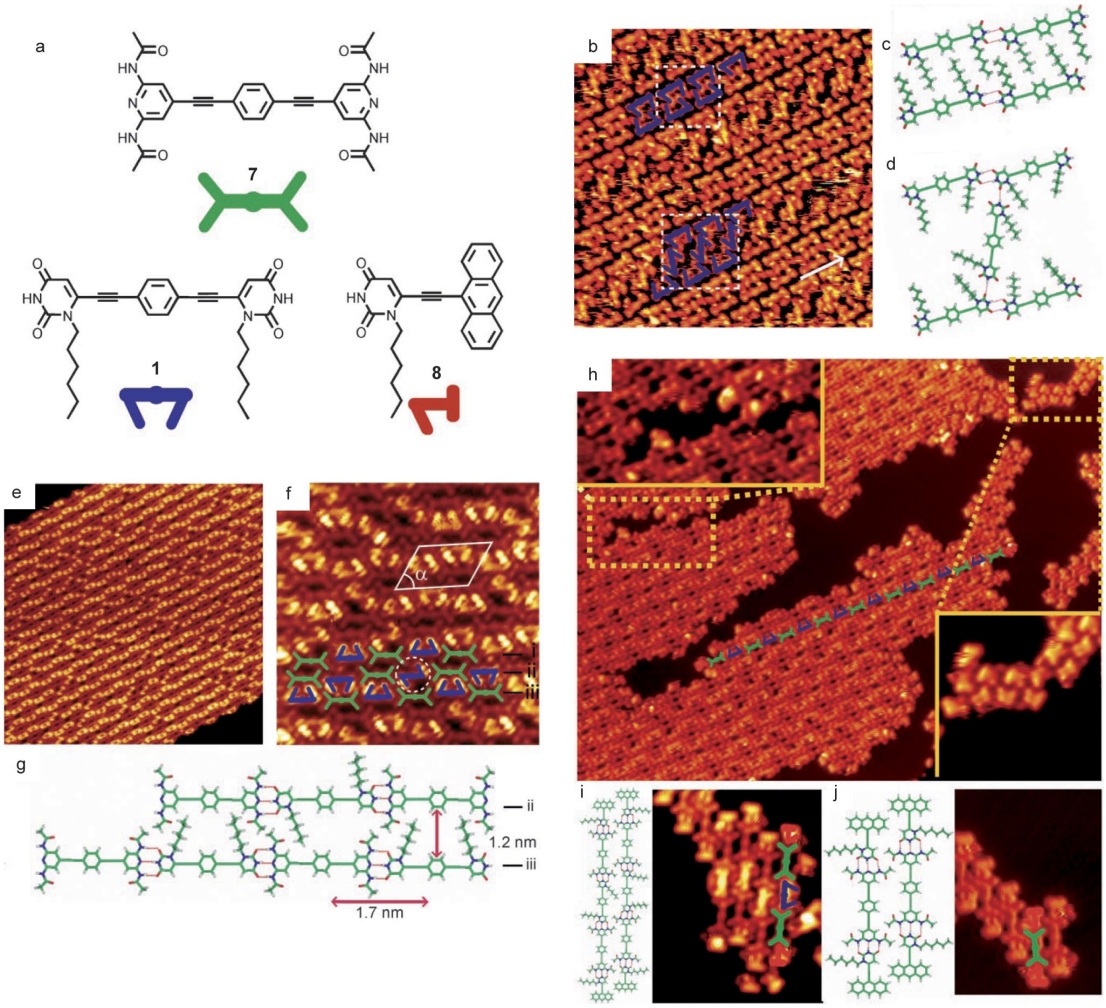

Fig. 5 (a) Chemical structures of the molecular modules used in the study; (b) STM image of the self-assembly of **1** on Ag(111) under UHV conditions (16×16 nm^2) and (c,d) the proposed models for the two types of packings; (e,f) STM images of the self-organized molecular wires formed by molecules **1** and **7** on Ag(111) under UHV conditions following annealing at 383 K (41.5×41.5 nm^2 and 12×12 nm^2, respectively) and (g) the proposed model for the linear molecular wire assembly; (h) STM image of the tricomponent submonolayer architecture formed upon sequential sublimation of **1**, **7**, and **8** onto Ag(111) under UHV conditions (50×40 nm^2). The lower right inset shows an aggregate of **8** (7.7×7.7 nm^2); (i,j) proposed models and zoom in STM image of trimeric and pentameric assemblies, respectively [54]. Adapted with permission from Wiley-VCH Verlag GmbH & Co. KGaA. Copyright © 2008.

in the absence of **8** (Figs. 5h–j). This was therefore the first example of a tricomponent miniature assembly. A mixture of short linear trimeric structures, [8·7·8] (Fig. 5j), pentameric structures, [8·7·1·7·8] (Fig. 5i) and long oligomers, [8·7·(1·7)n·8] (Fig. 5h) were observed by STM. Since **1** and **8** bear the same H-bonding motifs, they were expected to compete equally for interactions with **7**, however, clearly this was not the case since long oligomers predominated the assembly system. The reason for this is that the filling of empty space on the surface reduces the free surface energy which is the general tendency for any system on a surface [17]. Molecular stopper **8** does not allow such minimization in the occupied area per assembly as effectively as molecule **1**. This is because it only bears one

H-bonding moiety that is able to make energetically favored H-bonds compared to the two possessed by **1**. The anthracyl moiety can only interact via vdW interactions, however assemblies formed by these interactions are energetically less favored compared to H-bonding. The existence of voids within the intermixed regions (Fig. 5h, left dotted rectangle) and the formation of aggregates of **8** as small disordered islands (Fig. 5h, right dotted rectangle) support this hypothesis. Although precise control of the length of the molecular wires was not achieved in this study, it is postulated that by controlling the ratio of the molecular modules it could result in regular monodispersed self-assembling architectures on surfaces.

Self-assembly at liquid interfaces

Apart from these recent works on surfaces, we have also been able to demonstrate the utility of our the complementary H-bonding recognition in the formation of organized nanoscale structures in liquid media [55]. In this work (Fig. 6a), we have studied the self-assembly of molecular module **8** with alkoxy-bearing derivative **9** (long alkoxy chains were added to the central phenyl ring in order to enhance its solubility in nonpolar organic solvents) in cyclohexane by means of UV/vis absorption and emission spectroscopy as well as transmission electron microscopy (TEM) and AFM. Variable-temperature absorption and emission spectral changes of the individual molecules in cyclohexane indicated that molecule **9** undergoes reversible self-aggregation that is thought to be driven by a combination of weak homomolecular H-bonding, dipolar and π–π stacking interactions. Molecule **8**, on the other hand, showed small or no changes in the spectra, indicating that no aggregation was occurring. Next, the temperature effect on a mixture of two equivalents of **8** and one equivalent of **9** was investigated. The presence of a new red-shifted band in the absorption spectra at 470 nm, which disappears and reappears after respectively increasing and decreasing the temperature suggests that the formation of H-bonded supramolecular architectures form in cyclohexane and subsequently fosters the formation of π–π stacking aggregates of the resultant H-bonded architectures (this was further supported by Job plot titrations studies). In order to fully characterize the molecular assemblies, they were subjected to TEM and AFM analysis. Initially, a solution of molecule **9** was drop-casted onto a freshly cleaved mica surface and was imaged by both TEM and AFM techniques (Figs. 6b,e) in the absence of **8**. This resulted in the formation of both spherical micro- and nanoparticles (from ~10 nm to >1 μm), which are formed via the aforementioned intermolecular interactions. When a mixed solution of **8** and **9** was drop-casted onto mica with a 2:1 molar ratio, both TEM and AFM (Figs. 6c,f) indicated the formation of spherical vesicles of highly uniform size distribution (from 80 to 180 nm). Due to the H-bonding interactions allowing the passage from **9** to [**9**·(**8**)$_2$], there is a dramatic change in the end functionality properties of molecule **9**, going from solvophobic (in cyclohexane) in the absence of **8** to solvophilic. This consequently increases the solute–solvent interaction, which nurtures the formation of thermodynamically favored nanostructures with a narrow size distribution. Changing the equimolar (1:1) solution of the two molecular modules also resulted in formation of spherical nanoparticles, but with a larger size distribution (150–500 nm), presumably caused by the formation of various adducts of different stoichiometries exhibiting both solvophilic and solvophobic terminals (Figs. 6d,g).

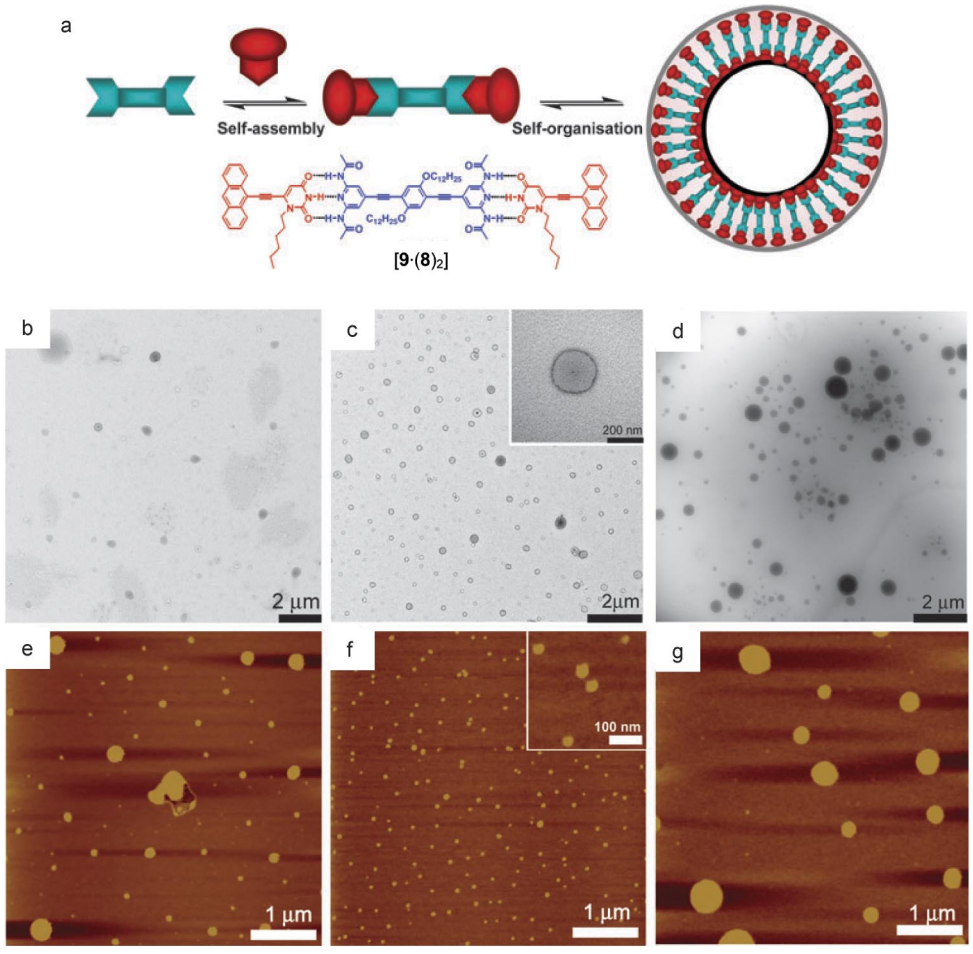

Fig. 6 (a) Chemical structures of **8** and **9**, as well as a schematic representation of the self-organization process between the two molecular modules; (b,e) TEM and AFM images, respectively, of the self-assembled structures of **9**; (c,f) TEM and AFM images, respectively, of the vesicular molecular adducts formed between **8** and **9** in a 2:1 ratio; (d,g) TEM and AFM images, respectively, of the molecular adducts formed between **8** and **9**, when in a 1:1 ratio. All nanostructures were deposited on freshly cleaved mica surfaces [55]. Adapted with permission from The Royal Society of Chemistry. Copyright © 2009.

CONCLUSIONS

In this account, we have described our recent strategies toward the preparation of nanostructured architectures via the self-assembly of organic molecular modules which were synthetically preprogrammed to exploit their H-bonding motifs in a predictable and reproducible manner. We have shown that utilizing a small library of related compounds a variety of nanostructured porous networks, arrays, and architectures can be prepared at various interfaces, including the solid–liquid, solid–vacuum, and liquid–liquid interfaces. The use of H-bonding supramolecular interactions proved to be an efficient approach to obtain well-ordered and defect-free nanopatterned materials in one and two dimensions. It should be noted that the examples described in this account are only our first steps toward the rational engineering and preparation of functional supramolecular architectures. Further developments on this early work should eventually lead to systems that could display functionality at the macroscopic level, enabling us to prepare future devices in fields such as information storage, displays, photovoltaics, con-

ductors, and even drug delivery. As we have also concluded in a previous report [36], these examples illustrate how the "bottom-up" approach is creeping ever closer toward the manufacture of technologies for the preparation of more complex and functional organic architectures.

ACKNOWLEDGMENTS

We thank the European Union through the Marie-Curie Research Training Network "PRAIRIES" (contract MRTN-CT-2006-035810), the Marie-Curie Initial Training Network "FINELUMEN" (grant agreement PITN-GA-2008-215399), the Belgian National Research Foundation (FRS-FNRS, contract MIS F.4505.10), the Région WALLONNE through the SOLWATT program (SUNTUBE, contract no. 850551), INSTM, the University of Trieste, and the University of Namur for the support provided for the completion of this work. Dr. H. Spillmann and Dr. M. Sthör (University of Basel, CH), Dr. T. Jung (Paul Scherrer Institut, CH), Dr. N. Armaroli (ISOF-CNR Bologna, IT), and Prof. P. Samorì (UDS Strasbourg, FR) are especially acknowledged for their fruitful collaboration and contribution throughout these years for our achievements on supramolecular H-bonded networks.

REFERENCES

1. E. H. Roderick, R. H. Williams. *Metal-Semiconductor Contacts*, Clarendon, Oxford (1998).
2. G. Ashkenasy, D. Cahen, R. Cohen, A. Shanzer, A. Vilan. *Acc. Chem. Res.* **35**, 121 (2002).
3. D. Cahen, G. Hodes. *Adv. Mater.* **14**, 789 (2002).
4. S. R. Forrest. *Nature* **428**, 911 (2004).
5. A. P. H. J. Schenning, E. W. Meijer. *Chem. Commun.* 3245 (2005).
6. J. E. Green, J. W. Choi, A. Boukai, Y. Bunimovich, E. Johnston-Halperin, E. DeIonno, Y. Luo, B. A. Sheriff, K. Xu, Y. S. Shin, H.-R. Tseng, J. F. Stoddart, J. R. Heath. *Nature* **445**, 414 (2007).
7. H. Haick, D. Cahen. *Acc. Chem. Res.* **41**, 359 (2008).
8. A. R. Murphy, J. M. J. Fréchet. *Chem. Rev.* **107**, 1066 (2007).
9. J. Wu, W. Pisula, K. Müllen. *Chem. Rev.* **107**, 718 (2007).
10. H. Yang, T. J. Shin, L. Yang, K. Cho, C. Y. Ryu, Z. Bao. *Adv. Funct. Mater.* **15**, 671 (2005).
11. A. Ajayaghosh, V. K. Praveen. *Acc. Chem. Res.* **40**, 644 (2007).
12. A. S. Arico, P. Bruce, B. Scrosati, J.-M. Tarascon, W. van Schalkwijk. *Nat. Mater.* **4**, 366 (2005).
13. F. Cacialli, J. S. Wilson, J. J. Michels, C. Daniel, C. Silva, R. H. Friend, N. Severin, P. Samorì, J. P. Rabe, M. J. O'Connell, P. N. Taylor, H. L. Anderson. *Nat. Mater.* **1**, 160 (2002).
14. R. H. Friend, R. W. Gymer, A. B. Holmes, J. H. Burroughes, R. N. Marks, C. Taliani, D. D. C. Bradley, D. A. D. Santos, J. L. Bredas, M. Logdlund, W. R. Salaneck. *Nature* **397**, 121 (1999).
15. Y. Yamamoto, T. Fukushima, Y. Suna, N. Ishii, A. Saeki, S. Seki, S. Tagawa, M. Taniguchi, T. Kawai, T. Aida. *Science* **314**, 1761 (2006).
16. D. Philp, J. F. Stoddart. *Angew. Chem., Int. Ed.* **35**, 1154 (1996).
17. G. M. Whitesides, J. P. Mathias, C. T. Seto. *Science* **254**, 1312 (1991).
18. J. E. Green, J. Wook Choi, A. Boukai, Y. Bunimovich, E. Johnston-Halperin, E. DeIonno, Y. Luo, B. A. Sheriff, K. Xu, Y. Shik Shin, H.-R. Tseng, J. F. Stoddart, J. R. Heath. *Nature* **445**, 414 (2007).
19. H. Haick, D. Cahen. *Acc. Chem. Res.* **41**, 359 (2008).
20. A. R. Murphy, J. M. J. Fréchet. *Chem. Rev.* **107**, 1066 (2007).
21. J. Wu, W. Pisula, K. Müllen. *Chem. Rev.* **107**, 718 (2007).
22. H. Yang, T. J. Shin, L. Yang, K. Cho, C. Y. Ryu, Z. Bao. *Adv. Funct. Mater.* **15**, 671 (2005).
23. L. Piot, C.-A. Palma, A. Llanes-Pallas, M. Prato, Z. Szekrényes, K. Kamarás, D. Bonifazi, P. Samorì. *Adv. Funct. Mater.* **19**, 1207 (2009).
24. D. L. Taylor, E. S. Woo, K. A. Giuliano. *Curr. Opin. Biotechnol.* **12**, 75 (2001).
25. M. Sarikaya, C. Tamerler, A. K. Y. Jen, K. Schulten, F. Baneyx. *Nat. Mater* **2**, 577 (2003).

26. J. V. Barth. *Annu. Rev. Phys. Chem.* **58**, 375 (2007).
27. J. V. Barth, G. Costantini, K. Kern. *Nature* **437**, 671 (2005).
28. D. Bonifazi, A. Kiebele, M. Stöhr, F. Cheng, T. Jung, F. Diederich, H. Spillmann. *Adv. Funct. Mater.* **17**, 1051 (2007).
29. F. Rosei. *J. Phys.: Condens. Matter* **16**, S1373 (2004).
30. F. Rosei, M. Schunack, Y. Naitoh, P. Jiang, A. Gourdon, E. Laegsgaard, I. Stensgaard, C. Joachim, F. Besenbacher. *Prog. Surf. Sci.* **71**, 95 (2003).
31. A. Ciesielski, G. Schaeffer, A. Petitjean, J.-M. Lehn, P. Samorì. *Angew. Chem., Int. Ed.* **48**, 2039 (2009).
32. D. M. Guldi, G. M. A. Rahman, F. Zerbetto, M. Prato. *Acc. Chem. Res.* **38**, 871 (2005).
33. F. J. M. Hoeben, P. Jonkheijm, E. W. Meijer, A. P. H. J. Schenning. *Chem. Rev.* **105**, 1491 (2005).
34. L. J. Prins, D. N. Reinhoudt, P. Timmerman. *Angew. Chem., Int. Ed.* **40**, 2382 (2001).
35. J. K. Gimzewski, C. Joachim. *Science* **283**, 1683 (1999).
36. D. Bonifazi, S. Mohnani, A. Llanes-Pallas. *Chem.—Eur. J.* **15**, 7004 (2009).
37. T. Kudernac, S. Lei, J. A. A. W. Elemans, S. De Feyter. *Chem. Soc. Rev.* **38**, 402 (2009).
38. P. Samorì. *J. Mater. Chem.* **14**, 1353 (2004).
39. J. A. A. W. Elemans, S. Lei, S. De Feyter. *Angew. Chem., Int. Ed.* **48**, 7298 (2009).
40. P. Samorì. *Chem. Soc. Rev.* **34**, 551 (2005).
41. J. A. A. W. Elemans, I. D. Cat, H. Xu, S. De Feyter. *Chem. Soc. Rev.* **38**, 722 (2009).
42. S. De Feyter, F. C. De Schryver. *Chem. Soc. Rev.* **32**, 139 (2003).
43. S. De Feyter, F. C. De Schryver. *J. Phys. Chem. B* **109**, 4290 (2005).
44. C. A. Palma, M. Bonini, A. Llanes-Pallas, T. Breiner, M. Prato, D. Bonifazi, P. Samorì. *Chem. Commun.* 5289 (2008).
45. C. A. Palma, J. Bjork, M. Bonini, M. S. Dyer, A. Llanes-Pallas, D. Bonifazi, M. Persson, P. Samorì. *J. Am. Chem. Soc.* **131**, 13062 (2009).
46. M. Bonini, L. Zalewski, T. Breiner, F. Dötz, M. Kastler, V. Schädler, M. Surin, R. Lazzaroni, P. Samorì. *Small* **5**, 1521 (2009).
47. C.-A. Palma, M. Bonini, T. Breiner, P. Samorì. *Adv. Mater.* **21**, 1383 (2009).
48. X.-H. Kong, K. Deng, Y.-L. Yang, Q.-D. Zeng, C. Wang. *J. Phys. Chem. C* **111**, 17382 (2007).
49. S. Lei, M. Surin, K. Tahara, J. Adisoejoso, R. Lazzaroni, Y. Tobe, S. De Feyter. *Nano Lett.* **8**, 2541 (2008).
50. M. Li, K. Deng, S.-B. Lei, Y.-L. Yang, T.-S. Wang, Y.-T. Shen, C.-R. Wang, Q.-D. Zeng, C. Wang. *Angew. Chem., Int. Ed.* **47**, 6717 (2008).
51. J. Adisoejoso, K. Tahara, S. Okuhata, S. Lei, Y. Tobe, S. De Feyter. *Angew. Chem., Int. Ed.* **48**, 7353 (2009).
52. A. Llanes-Pallas, C. A. Palma, L. Piot, A. Belbakra, A. Listorti, M. Prato, P. Samorì, N. Armaroli, D. Bonifazi. *J. Am. Chem. Soc.* **131**, 509 (2009).
53. M. Matena, A. Llanes-Pallas, M. Enache, T. Jung, J. Wouters, B. Champagne, M. Stöhr, D. Bonifazi. *Chem. Commun.* 3525 (2009).
54. A. Llanes-Pallas, M. Matena, T. Jung, M. Prato, M. Stöhr, D. Bonifazi. *Angew. Chem., Int. Ed.* **47**, 7726 (2008).
55. K. Yoosaf, A. Belbakra, N. Armaroli, A. Llanes-Pallas, D. Bonifazi. *Chem. Commun.* 2830 (2009).

